CATHODIC ELECTRODEPOSITION OF Cu_4SnS_4 THIN FILMS FROM ACIDIC SOLUTION

Anuar Kassim*[1], Ho Soon Min[1], Zulkefly Kuang[1], Tan Wee Tee[1], Abdul Halim Abdullah, Atan Sharif[1], Md. Jelas Haron[1] and Saravanan Nagalingam[2]

[1]Department of Chemistry, Faculty of Science,
Universiti Putra Malaysia, 43400 Serdang, Selangor, Malaysia
[2]Department of Bioscience and Chemistry, Faculty of Engineering and Science,
Universiti Tunku Abdul Rahman, 53300 Kuala Lumpur, Malaysia

Corresponding author. Tel: +60389466779, Fax: +60389435380
E-mail address: anuar@fsas.upm.edu.my

ABSTRACT

In this work the synthesis of copper tin sulfide thin films by electrodeposition is carried out. The films were deposited onto ITO glass substrates from an aqueous solution bath containing copper sulfate, tin chloride and sodium thiosulfate at pH 1 and room temperature. Prior to the deposition, a cyclic voltammetry experiment was carried out between two potential limits (+1000 to -1000 mV versus Ag/AgCl) to probe the effect of the applied potential and to determine the most likely suitable electrodeposition potential for the deposition of copper tin sulfide. The deposition was attempted at various cathodic potentials such as -400, -600, -800, -1000 mV to determine the optimum deposition potential. The films have been characterized by techniques such as optical absorption, X-ray diffraction and atomic force microscopy. The XRD patterns show that the films are polycrystalline with orthorhombic structure. The AFM studies reveal the electrodeposited films were smooth, compact and uniform at deposition potentials of –600 mV versus Ag/AgCl. The direct optical band-gap energy was obtained to be 1.58 eV.

Keywords: Electrodeposition; Cyclic voltammetry; Thin films; Semiconducting material

1. INTRODUCTION

The solar cell is considered a major candidate for obtaining energy from the sun, since it can convert sunlight directly to electricity. Recently, the use of photoelectrochemical solar cells leads to a large amount of research on the search for metal chalcogenides thin film with acceptable efficiency. Ternary chalcogenides have potential application in solar energy conversion[1-9]. There are many methods for preparing ternary chalcogenide thin films such as chemical bath deposition[10], electrodeposition[11], electrochemical atomic layer epitaxy[12], flash evaporation[13], electron bean evaporation[14], spray pyrolysis[15], sputter deposition[16], thermal evaporation[17] and vacuum evaporation[18]. Amongst these deposition methods, electrodeposition is more attractive, since it offers the advantages of simple,

economy, convenience and several experimental parameters can be controlled more precisely. In this paper, we study the voltammetric behavior of the copper tin sulfide on indium tin oxide glass substrate from aqueous solutions. The thin films were prepared by electrodeposition at different deposition potentials. We investigated the influence of the deposition potential on the optical properties, morphological and structural of electrodeposited thin films by using UV-Visible Spectrophotometer, atomic force microscopy and X-ray diffraction, respectively.

2. EXPERIMENTAL PROCEDURE

The deposition bath contains copper sulfate ($CuSO_4$), tin chloride ($SnCl_2.2H_2O$) and sodium thiosulfate ($Na_2S_2O_3.5H_2O$). All the reagents used were of analytical grade. The pH of the solution was adjusted to 1 by using HCl. Films were deposited using a three electrode cells. The Bioanalytical System BAS 100W Electrochemical Analyzer was employed for recording the cyclic voltammograms and controlling the deposition potentials. The electrodes were an indium doped tin oxide glass substrate as a working electrode, a platinum wire as a counter electrode and a silver-silver chloride as the reference electrode. The substrates were cleaned ultrasonically in water and ethanol before use. Purified nitrogen was flowed into the deposition bath for few minutes to create oxygen free environment. In order to determine the optimum condition, the films were deposited in various deposition potentials (–400 mV, -600mV, -800 mV and –1000 mV versus Ag/AgCl). Upon deposition the deposits was rinsed with distilled water and kept for further analysis. X-ray diffraction (XRD) analysis was carried out using a Philips PM 11730 diffractometer for the 2θ ranging from 20° to 60° with CuK_α (λ=1.5418 Å) radiation. Topography was measured by using an atomic force microscopy (Quesant Instrument Corporation, Q-Scope 250) operating in contact mode, with a commercial Si_3N_4 cantilever. Optical absorption study was carried out using the Perkin Elmer UV/Vis Lambda 20 Spectrophotometer. The film-coated ITO glass was placed across the sample radiation pathway while the uncoated ITO glass was put across the reference path. The absorption data were manipulated for the determination of the band gap energy, E_g.

3. RESULTS AND DISCUSSION

3.1 Cyclic voltammetry

Cyclic voltammetry was used to monitor the electrochemical reactions in solutions in $SnCl_2.2H_2O$, $CuSO_4$ and $Na_2S_2O_3.5H_2O$ respectively, then in their combined solution of the same concentration and pH (Figure 1a-d). Figure 1a shows the voltammogram recorded for tin chloride on ITO glass substrate. The forward scan shows a reduction potential starting at about –500 mV. This is due to the reduction process of tin onto the working electrode. The reduction peak increases towards the more negative region where hydrogen evolution also occurs. During the reverse scan, the oxidation wave of tin could be seen starting at about –450 mV. This peak reaches a maximum value of about –200 mV. This oxidation peak clearly shows the process is reversible whereby the deposited

tin dissolves upon reversing the potential. In the case of copper sulfate solution (Figure 1b), the current rise started at −50 mV followed by large reduction wave at −500 mV. This response is associated with Cu (II) reduction on ITO substrate. The deposition reaction is reconfirmed by the reverse scan. The two stripping peaks at positive potential limits, 200-600 mV indicated the oxidation of the copper compound.


(a)

(b)

(c)

(d)
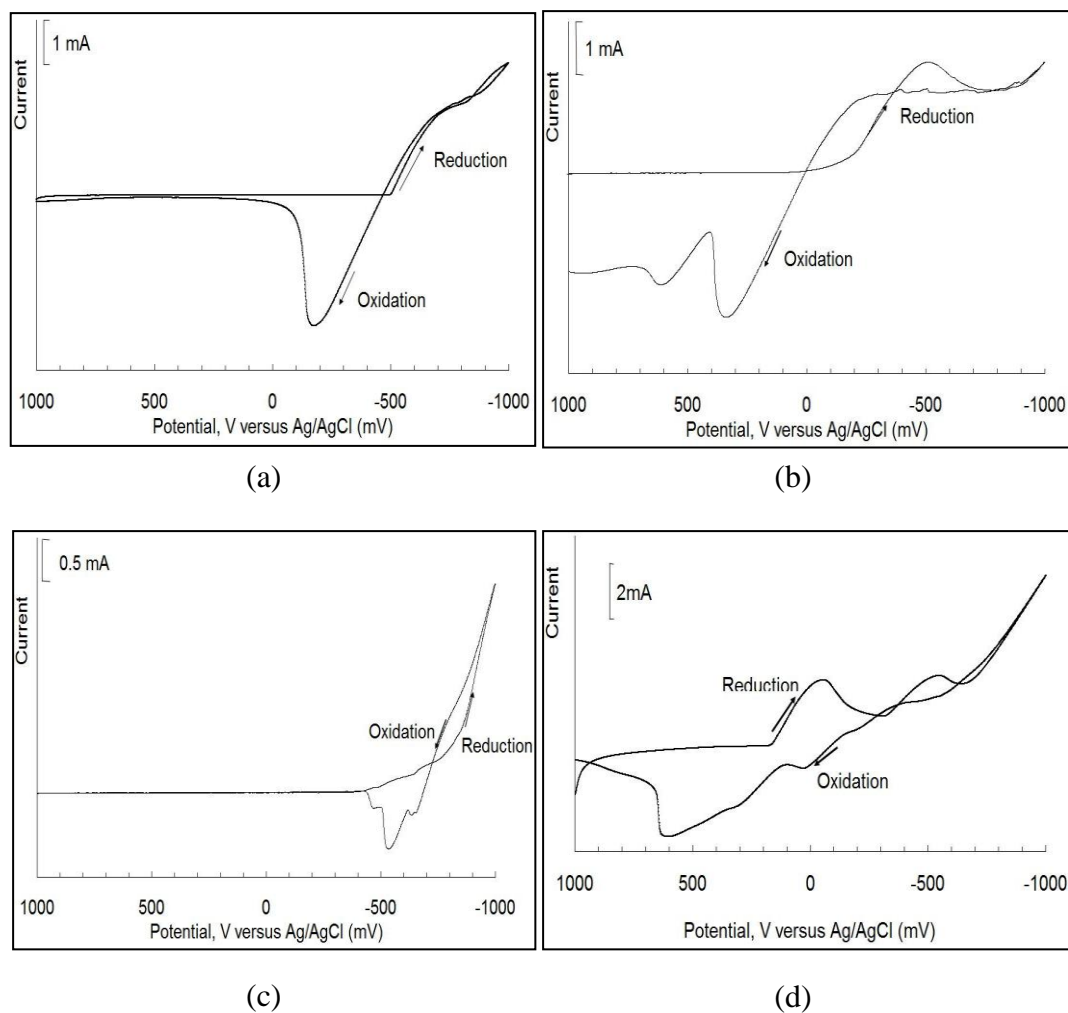
Figure 1: *Cyclic voltammogram of (a) 0.01M SnCl$_2$.2H$_2$O (b) 0.01 M CuSO$_4$ (c) 0.01 M Na$_2$S$_2$O$_3$.5H$_2$O (d) mixture of SnCl$_2$.2H$_2$O, CuSO$_4$ and Na$_2$S$_2$O$_3$.5H$_2$O solutions at room temperature, scan rate: 10 mV/s and pH 1.*

The forward scan of sodium thiosulfate solution (Figure 1c) shows the cathodic current starts flowing at about −500mV. The shoulder at −700 mV may be associated with the reduction of thiosulphate ions. This reduction wave may be due to the S$_2$O$_3^{2-}$ ions released during the disproportion of Na$_2$S$_2$O$_3$ at the pH of 1.0. Figure 1d shows the cyclic voltammogram of the ITO working electrode in the mixture of copper sulfate, tin chloride

and sodium thiosulfate. The wave around –475 mV corresponds to the formation of Cu_4SnS_4 layers and the cathodic current increases gradually up to –1000 mV indicating the growth of layers. The anodic peak around 54 mV corresponds to the stripping of deposited layers in the reverse scan. Based on the above results, the voltammogram suggested that a deposition on the working electrode can be expected when the potentials above –500mV are applied.

3.2 XRD analysis

Figure 2 shows the XRD pattern for the films deposited at various deposition potentials. Four main peaks at 2θ =30.3°, 35.5°, 45.2° and 50.6° corresponding to d-spacing values 2.95, 2.55, 2.00 and 1.80 Å which attributed to the (221), (420), (512) and (711) planes, respectively are detected from all the samples. These observed d spacing values and the standard values are in good agreement with the Joint Committee on Powder Diffraction Standards values (Reference code: 010710129) in Table 1 that showed the highest peak at 2.95Å corresponding to (221) plane. Raising the deposition potential further to –800mV and more negative of values, however, resulted in the disappearance of the plane (022) and some new peaks gradually could be observed. The new peaks corresponding to sulfur (Reference code: 010740791) could be observed at -1000 mV.
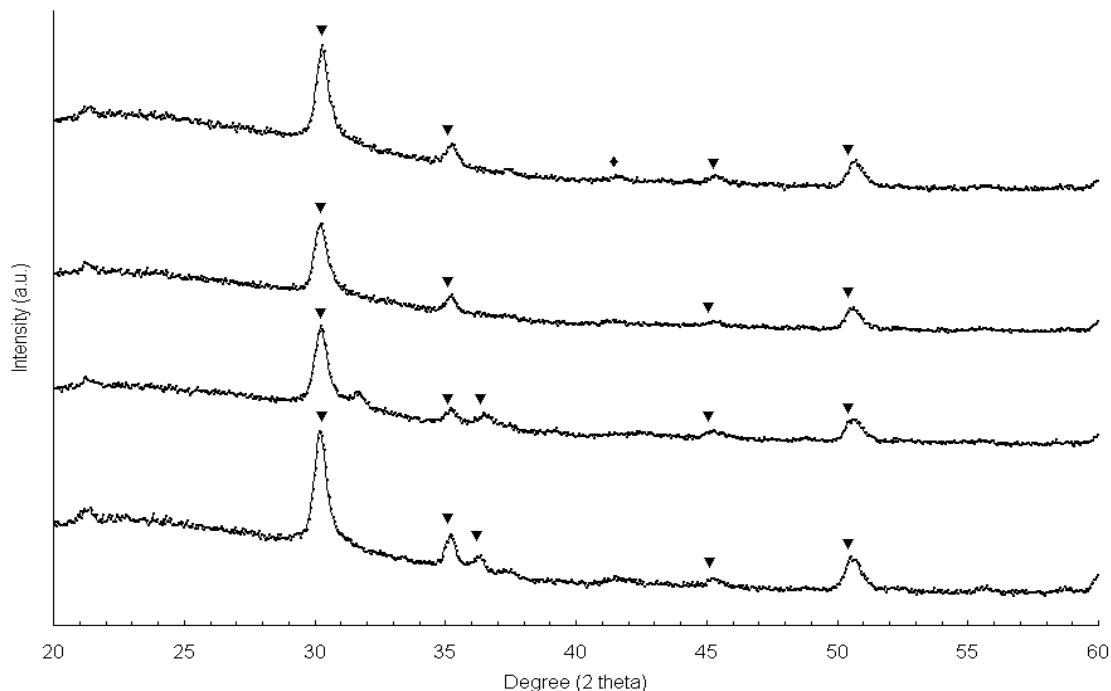
***Figure 2:*** *X-ray diffraction pattern of samples prepared at different deposition potentials* Cu_4SnS_4 *(▼)* S_{12} *(♦)*

Table 1: *Comparison between observed d spacing values of Cu_4SnS_4 at different deposition potential with JCPDS data*

Deposition potential (versus Ag/AgCl)	2θ (°)	d-spacing		$h\,k\,l$	Compounds
		Observed values (Å)	JCPDS data (Å)		
-400 mV	30.2	2.96	2.96	221	Cu_4SnS_4
	35.2	2.55	2.54	420	Cu_4SnS_4
	36.4	2.47	2.46	022	Cu_4SnS_4
	45.2	2.01	2.00	512	Cu_4SnS_4
	50.5	1.81	1.80	711	Cu_4SnS_4
-600 mV	30.2	2.96	2.96	221	Cu_4SnS_4
	31.7	2.82	2.82	103	CuS
	35.2	2.55	2.54	420	Cu_4SnS_4
	36.5	2.46	2.46	022	Cu_4SnS_4
	45.2	2.00	2.00	512	Cu_4SnS_4
	50.6	1.80	1.80	711	Cu_4SnS_4
-800 mV	30.2	2.96	2.96	221	Cu_4SnS_4
	35.2	2.55	2.54	420	Cu_4SnS_4
	45.3	2.00	2.00	512	Cu_4SnS_4
	50.6	1.80	1.80	711	Cu_4SnS_4
-1000 mV	30.3	2.95	2.96	221	Cu_4SnS_4
	35.3	2.54	2.54	420	Cu_4SnS_4
	41.6	2.17	2.17	125	S_{12}
	45.4	2.00	2.00	512	Cu_4SnS_4
	50.6	1.80	1.80	711	Cu_4SnS_4

3.3 AFM analysis

The surface images in an area of 10 μm X 10 μm of the thin films deposited at various deposition potential values are shown in Figure 3. It can be observed that the surface of the films is not very compact (Figure 3a). The films are constituted by micro particles with an irregular size distribution. A lot of empty spaces can be seen between these micro particles.

The AFM images of samples clearly show the conversion of micro particles into spherical grains that were quite uniform over the entire glass substrate (Figure 3b). However, it is seen from the intensity distribution that the film consists of smaller and larger micro particles in deposition potential above –800 mV (Figure 3c,d). At the right hand side of the image, intensity strip is shown which indicates the height of the surface grain along Z-axis. AFM picture shows the presence of high hills on top of a homogeneous granular background surface. The height of the hills is found decreased as the deposition potential increases.

(a)   (b)

(c)   (d)
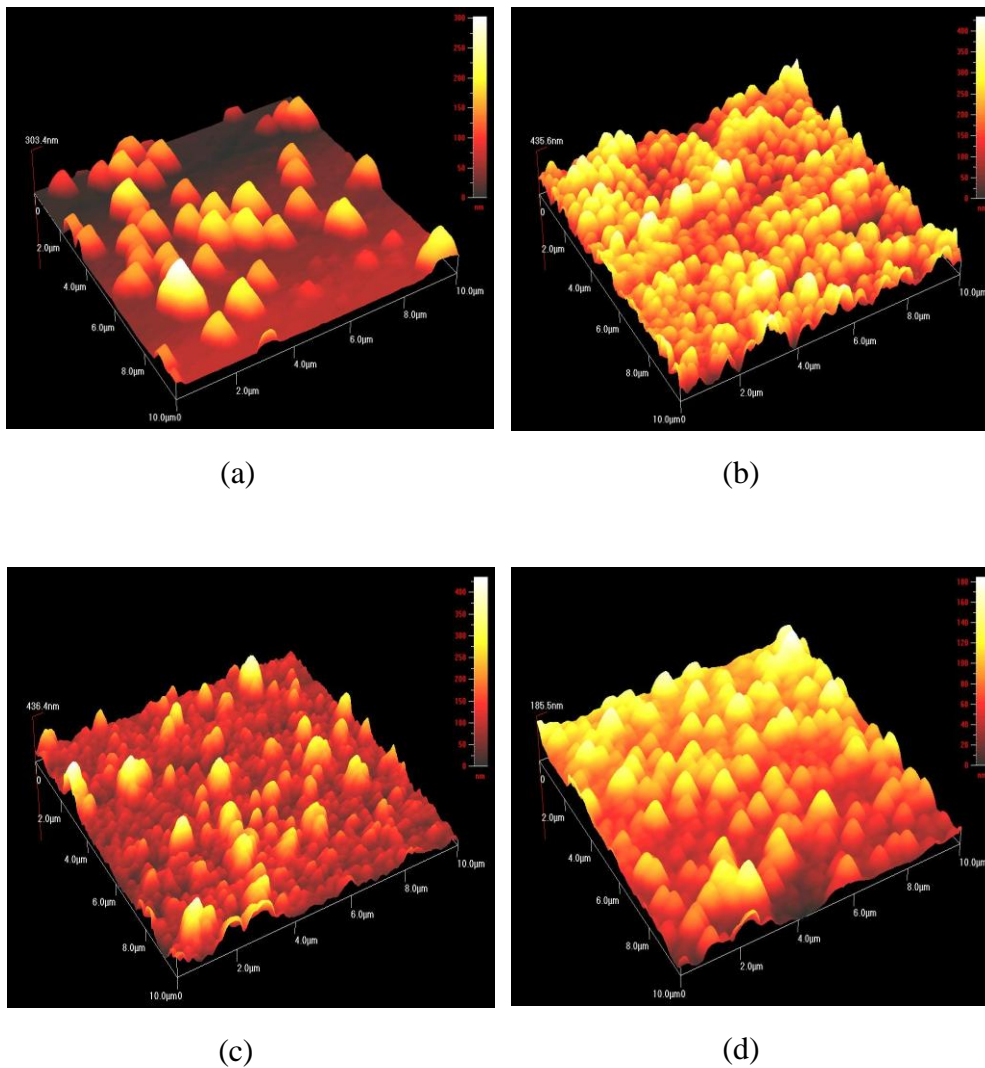
Figure 3: *Atomic force microscopy images of Cu_4SnS_4 thin films at different deposition potentials (versus Ag/AgCl)*
(a) –400 mV (b) –600 mV (c) –800 mV (d) –1000 mV

3.4 Optical properties

Deposition was carried out on an ITO glass substrate to study the optical behavior of the Cu_4SnS_4 films. Figure 4 shows the optical absorbance data of the films versus wavelength obtained from UV-Visible spectrophotometer. The absorption could be observed between 300 to 800 nm. The spectrum shows a gradually increasing absorbance throughout the visible region for all samples, which makes it possible for this material to be used in a photoelectrochemical cells. The absorbance of thin films deposited at –600 mV produced

higher absorbance value. However, it is seen from figure that as the deposition potential increases (above –800 mV), the absorbance value decreases.
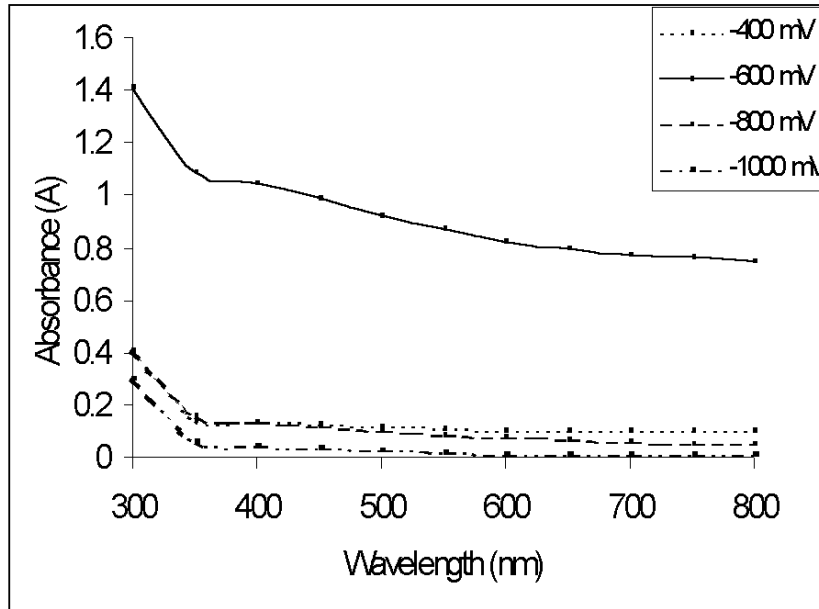

Figure 4: *Absorbance versus wavelength spectra for Cu₄SnS₄ films deposited at different deposition potentials (versus Ag/AgCl)*

The band gap energy and transition type was derived from mathematical treatment of data obtained from optical absorbance versus wavelength with the following relationship for near-edge absorption:

$$A = \frac{[k(hv - E_g)^{n/2}]}{hv}$$ ……………………………………………………..(1)

where v is the frequency, h is the Planck's constant, k equals to constant while n carries the value of either 1 or 4. The value of n is 1 and 4 for the direct transitions and indirect transitions, respectively. The band gap, E_g, could be obtained from a straight line plot of $(Ahv)^{2/n}$ as a function of hv (Figure 5). Extrapolation of the line to the base line, where the value of $(Ahv)^{2/n}$ is zero, will give E_g.

The straight-line plot in Figure 5b (with a correlation factor for straight line fit of 0.975) indicating that the energy band gap of Cu₄SnS₄ is direct transition and yield a band gap of 1.58eV. Table 2 lists the direct band gap for the Cu₄SnS₄ thin films deposited at different deposition potentials. The direct band gap energy of the thin films initially decreases (1.61 to 1.58 eV) with increasing the cathodic potential from –400mV to –600 mV. Subsequently, further increasing in deposition potential (more negative than –800 mV) caused increasing the band gap energy. Therefore, the deposition potential has some influence on the band gap of the films.

(a)

(b)

(c)

(d)
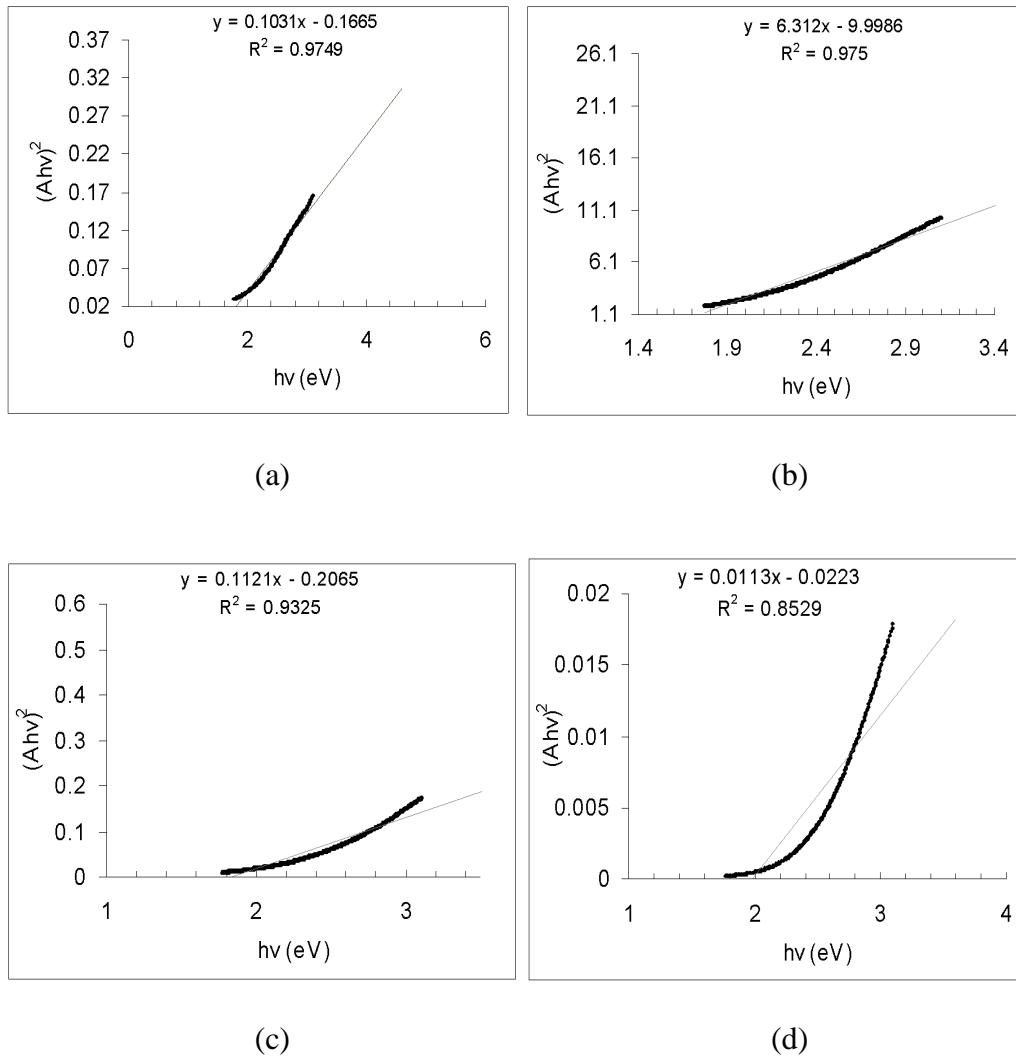
Figure 5: *Plot of $(Ahv)^{2/n}$ versus hv for deposited thin films at different deposition potentials (n = 1)*
(a) –400 mV (b) –600mV (c) –800 mV (d) –1000 mV

Table 2: *The direct band gap energy for the Cu_4SnS_4 films deposited at different deposition potentials*

Deposition potential (versus Ag/AgCl)	Direct transition (eV)
-400 mV	1.61
-600 mV	1.58
-800 mV	1.84
-1000 mV	1.97

4. CONCLUSIONS

Cu_4SnS_4 thin films cathodically electrodeposited on an indium tin oxide glass substrate were found to be orthorhombic structure established by their XRD patterns. Decreasing in deposition potential resulted in an increase in the size of the grains and caused in growth of spherical particles. The film was found to exhibit direct transition in the visible spectrum with a bandgap value of about 1.58 eV at –600 mV. The film deposited at –600 mV showed higher absorption characteristics when compared to the film prepared at other deposition potentials. This result correlates well with the information obtained from the XRD, AFM, which shows good film formation at this potential.

ACKNOWLEDGEMENTS

REFERENCES

1. Hou, X.H. and Choy, K.L. (2005), Synthesis and characteristics of $CuInS_2$ films for photovoltaic application, Thin Solid Films, vol. 480-481, pp. 13-18

2. Shao, L.S., Chang, K.H. and Hwang, H.L. (2003), The one-step vacuum growth of high-quality $CuInS_2$ thin film suitable for photovoltaic applications, Mate. Sci. Semicond. Process., vol. 6(5-6), pp. 397-400

3. Asenjo, B., Chaparro, A.M., Gutierrez, M.T. and Herrero, J. (2006), Electrochemical growth and properties of $CuInS_2$ thin films for solar energy conversion, Thin Solid Films, vol. 511-512, pp. 117-120

4. Allen, M. H., Richard, W. and Rikard, W. (1998), Low-cost deposition of $CuInSe_2$ (CIS) films for CdS/CIS solar cells, Sol. Energy Mat. Sol. Cells, vol. 52(3-4), pp. 355-360

5. Park, G.C., Chung, H.D., Kim, C.D., Park, H.R., Jeong, W.J., Kim, J.U. and Lee, K.H. (1997), Photovoltaic characteristics of $CuInS_2$/CdS solar cell by electron beam evaporation, Sol. Energy Mat. Sol. Cells, vol. 49(1-4), pp. 365-374

6. Lewerenz, H.J. (2004), Development of copperindiumdisulfide into a solar material, Sol. Energy Mat. Sol. Cells, vol. 83(4), pp.395-407

7. Berenguier, B. and Lewerenz, H.J. (2005), Efficient solar energy conversion with electrochemically conditioned $CuInS_2$ thin film absorber layers, Electrochem. Commun, vol. 8, pp. 165-169

8. Vidyadharan, P.K. and Vijayakumar, K.P. (1998), Characterization of $CuInSe_2$/CdS thin-film solar cells prepared using CBD, Sol. Energy Mat. Sol. Cells, vol. 51, pp. 47-54

9. Subramanian, B., Sanvuraja, C. and Jayachandran, M. (2003), Materials properties of electrodeposited SnS0.5Se0.5 films and characterization of photoelectrochemical solar cells, Mater. Res. Bull., vol. 38, pp. 899-908

10: Ng, G. and Gaewdang, T. (2005), Investigations on chemically deposited $Cd_{1-x}Zn_xS$ thin films with low Zn content, Materials Letters, vol. 59, pp. 3577-3584

11. Dalchiele, E.A. Cattarin, S. and Musiani, M.M. (1998), Preparation of $CdIn_2Se_4$ thin films by electrodeposition, J. Appl. Electrochem., vol. 28, pp.1005-1008

12. Innocenti, M., Cattarin, S., Loglio, F., cecconi, T., seravalli, G. and Foresti, M.L. (2004), Ternary cadmium and zinc sulfides: composition, morphology and photoelectrochemistry, Electrochim Acta, vol. 49, pp.1327-1337

13. Sakata, H. and Ogawa, H. (2000), Optical and electrical properties of flash-evaporated amorphous $CuInSe_2$ films, Sol. Energy Mat. Sol. Cells, vol. 63, pp. 259-265

14. Islam, R. Banerjee, H.D. and Rao, R.D. (1995), Structural and optical properties of $CdSe_xTe_{1-x}$ thin films grown by electron beam evaporation, Thin Solid Films, vol. 266, pp. 215-218

15. Krunks, M., Kijatkina, O., Rebane, H., Oja, I., Mikli, V. and Mere, A. (2002), Composition of $CuInS_2$ thin films prepared by spray pyrolysis, Thin Solid films vol. 403-404, pp.71-75

16. He, Y.B., Polity, A., Alves, H.R., Osterreicher, I., Kriegseis, W., Pfistere, D., Meyer, B.K. and Hardt, M. (2002), Structural and optical characterization of RF reactively sputtered $CuInS_2$ thin films, Thin Solid Films, vol. 403-404, pp. 62-65

17. Qasrawi, A.F., Kayed, T.S. and Ercan, I. (2004), Fabrication and some physical properties of $AgIn_5S_8$ thin films, Materials Science and Engineering B, vol. 113, pp.73-78

18. Zribi, M., Rabeh, M.B., Brini, R., Kanzari, M. and Rezig, B. (2006), Influence of Sn incorporation on the properties of $CuInS_2$ thin films grown by vacuum evaporation method, Thin Solid Films, vol. 511-512, pp. 125-129